Second order thermal corrections to electron wavefunction

Mahnaz Q. Haseeb [a,*], Samina S. Masood [b]

[a] *Department of Physics, COMSATS Institute of Information Technology, Islamabad, Pakistan*
[b] *Department of Physics, University of Houston Clear Lake, Houston, TX 77058, United States*

A B S T R A C T

Second order perturbative corrections to electron wavefunction are calculated here, for the first time, at generalized temperature. Calculations of electron self energy are important for the renormalizability of electron mass and wavefunction in QED through order by order cancellation of singularities up to order α^2. Cancellation of temperature dependent singularities is demonstrated by incorporating the results of both orders of integration between cold and hot loops. For finite terms, we have rewritten second order thermal corrections as well, in a concise form, to calculate wavefunction renormalization constant. Our results are in a form that includes intermediate temperatures $T \sim m$ (where m is electron mass) while limits of high temperature $T \gg m$ and low temperature $T \ll m$ are also retrievable from them. A comparison with the existing results is included as well. The renormalized mass and wavefunction are used to calculate particle processes in extremely hot systems such as stellar cores and primordial nucleosynthesis during very early universe. An application to the latter case is also discussed.

© 2011 Elsevier B.V. All rights reserved.

1. Introduction

Finite temperature effects are applicable to extremely high temperature backgrounds, such as those that were present during primordial nucleosynthesis in the early universe and exist in astrophysical environments, etc. These effects are significant enough and should not be ignored in comparison with the vacuum contribution. High temperature and density effects in ultra-relativistic plasma are required to be incorporated in exceptionally hot early universe and hot and dense systems such as those in supernovae and cores of neutron stars. More recently renewed interest in hot and dense QED plasmas has been generated due to possibility of creating ultra-relativistic electron-positron plasmas with high-intensity lasers ($\approx 10^{18}$ W/cm^2) [1–3]. Two opposite laser pulses hitting a thin gold foil can heat up electrons in the foil up to several MeV ($\sim 10^{10}$ K).

Particles propagating in vacuum can be assumed to be the ones with interactions switched off. When these particles propagate through a medium, several kinds of interaction processes take place. This makes the properties of the system different from that in which all the particles are assumed to be completely independent of each other, behaving as freely propagating bare particles. When dealing with extremely hot environments in QED, where the particles propagate in statistical background at energies around the thresholds for particle–antiparticle pair production, temperature effects need to be appropriately taken into account. Such effects arise due to continuous electron and photon exchanges between particles during physical interactions that take place in a heat bath containing hot particles and antiparticles. The net statistical effects of background electrons and photons enter the theory through the fermion and boson distributions respectively.

Thermal background effects are included through radiative corrections [4,5]. Self energies, self masses and wavefunctions of the propagating particles acquire temperature corrections in this environment due to exchanges of energy and momentum with real particles. An exact state of all these background particles is unknown since they regularly fluctuate between different configurations and for this statistical approach is incorporated. Finite temperature calculations also provide a guideline to estimate density corrections at higher order loops through chemical potential effects of the background plasma.

Finite temperature propagators in real time formalism comprise of temperature dependent terms added to the particle propagators in vacuum theory [6]. In finite temperature electrodynamics, electric fields are further screened due to such interactions. Temperatures of interest in such a situation are in the range of a few MeV. Big Bang Nucleosynthesis (BBN) theory, together with precise Wilkinson

---

* Corresponding author.
E-mail address: mahnazhaseeb@comsats.edu.pk (M.Q. Haseeb).

Microwave Anisotropy Probe (WMAP) data for cosmic baryon density, leads to tight predictions for light elemental abundances after the big bang. The electron mass shifts determined through self energy corrections have relevance in primordial nucleosynthesis since they lead to modifications to neutron lifetime and hence helium (^{4}He) abundance parameter. Therefore electron self energy loops need to be evaluated with higher order corrections with more accuracy.

In literature, ways to compute finite temperature effects on phase-space, vertex, mass corrections and photon emission or absorption [7–16] are extensively discussed. Finite temperature wave function renormalization has been dealt with several approaches [9–18], specifically in the context of weak decay rates during primordial nucleosynthesis. They agree on using finite temperature Dirac spinors to obtain corresponding effective projection operator. Differences in the spinors presented in Refs. [17] and [18] were also pointed out [19]. However, their results in case of β-decay and related processes agreed with the ones obtained using the approaches that had already existed for wave function renormalization, except in case of a scalar boson decay into fermion–antifermion pair.

Real time formalism for calculations at finite temperature [20], provides an ease of obtaining the temperature corrections as additive terms to usual contribution in vacuum. We have used this formulation for calculation of electron self energy as a second order perturbative correction in α. From the self energy expression wavefunction renormalization is obtained, for the first time, in a generalized form such that intermediate temperatures $T \sim m$ are also included while the ranges of high temperature $T \gg m$ and low temperature $T \ll m$, are retrieved from them as the limiting cases. We have to rewrite the previously calculated self-mass of electron in a convenient form to be able to calculate wavefunction renormalization constant at the two loop level. We evaluate the loops with temperature dependent momenta integrated before temperature independent variables and vice versa, in the relevant order α^2 loops in QED, and compare these with the calculations of electron self energy done in Refs. [21,22] earlier. These results of loop integrations makes the calculations of loop momenta much more simpler and easier to handle.

Section 2 is based on the reexamined and simplified calculations of loop correction up-to two orders in α that contribute to electron self energy in this background. The electron mass shift and its relevance to the ^{4}He abundance parameter at the time of primordial nucleosynthesis is presented in Section 4. The wavefunction renormalization constant is calculated in Section 4 from self energy of electron up to the two loop level. Section 5 comprises of summary of the results.

2. Loop corrections to electron self energy

At one loop level, Feynman diagrams are calculated in usual way by substituting the propagators for electron, positron and photon in vacuum by those at finite temperature. Hot terms correspond to a contribution of real background particles on mass-shell that are in thermal equilibrium. In real time formalism, finite temperature terms remain separate at order α since terms depending on temperature (hot) are additive to temperature independent (cold) terms, in the propagators. Therefore, at one loop level the hot and cold loop momenta are integrated separately. However, in finite temperature field theory, covariance is maintained in real time framework at the cost of broken Lorentz invariance. This invariance is then inserted by hand through a choice of four velocity of the heat bath $u^\mu = (1, 0, 0, 0)$, that affects energy integrations in the loops.

Due to interactions with the background, electron and positron masses are known to get enhanced at one-loop and higher loop levels [4–9]. Photons also acquire dynamically generated mass due to plasma screening effect [23,24]. The presence of effective mass implies the fact that propagating particles constantly interact with the background. Radiatively generated thermal mass leads to a mass shift in physical quantities. This mass acts as a kinematical cut-off for physical processes, e.g., while determining production rate of particles in the heat bath.

Higher order loop corrections are required to study the perturbative behavior at finite temperature. Two loop integrals comprise of a combination of cold and hot momenta which appear due to an overlap of temperature dependent and temperature independent terms in the particle propagators. Therefore higher loop integrations involve an overlap of finite and divergent terms due to which these become analytically more complicated, even at the two loop level [24]. Integration of thermal integrals is done here before the temperature independent integrals and vice versa, in the rest frame of heat bath. One of the reasons for this is that there is a need to get rid of hot divergences appearing due to the presence of hot loops.

Renormalization in finite temperature field theories becomes somewhat different from that at zero temperature due to additional hot infrared divergences at finite temperature. These divergences get removed in particle decay processes via bremsstrahlung emission and absorption effects [5,25]. Temperature itself, however, acts as a regularization parameter for hot ultraviolet divergences. The order by order cancellation of singularities can be observed through an addition of all the diagrams of same order in α. Order α self energy determined for all the possible ranges of temperature valid in QED including $T \sim m$ was presented [25] as:

$$\Sigma_\beta(p) = \Sigma_{T=0}(p) + \frac{\alpha}{4\pi^2}\left[(\not{p} - m)I_A + \not{J} + (2m - \not{p})J_A + \not{J}_B\right] \tag{1}$$

where

$$I_A = 8\pi \int_0^\infty \frac{dk}{k} n_B(k), \qquad \frac{I^0}{E} = -\frac{2\pi^3 T^2}{3E^2 v} \ln\frac{1-v}{1+v}, \qquad \frac{\mathbf{I} \cdot \mathbf{p}}{\mathbf{p}^2} = -\frac{2\pi^3 T^2}{3E^2 v^3}\left\{\ln\frac{1-v}{1+v} + 2v\right\},$$

with $v = \frac{|\mathbf{p}|}{p_0}$, $(p_0 = E)$,

$$J^A \simeq -8\pi b(m\beta), \qquad \frac{J_B^0}{E} \simeq 4\pi\left[\frac{T}{E^2 v}\ln\frac{1+v}{1-v}\{ma(m\beta) - Tc(m\beta)\} - 3b(m\beta)\right],$$

$$\frac{\mathbf{J}_B \cdot \mathbf{p}}{\mathbf{p}^2} \simeq \frac{\pi}{v^2 E^2}\left[\left\{E^2 - \frac{2}{3}m^2\right\}b(m\beta) + 4T\left\{\frac{1}{v}\ln\frac{1+v}{1-v} + 2\right\}\{ma(m\beta) - Tc(m\beta)\}\right],$$

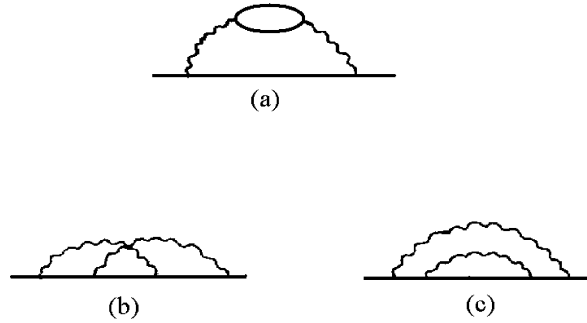**Fig. 1.** Two loop electron self energy diagrams.

$$a(m\beta) = \ln(1 + e^{-m\beta}), \qquad b(m\beta) = \sum_{n=1}^{\infty} (-1)^n \, \mathrm{Ei}(-nm\beta), \qquad c(m\beta) = \sum_{n=1}^{\infty} (-1)^n \frac{e^{-nm\beta}}{n^2},$$

and $\mathrm{Ei}(-x)$ is an error integral given by

$$\mathrm{Ei}(-x) = -\int_x^{\infty} \frac{dt}{t} e^{-t}.$$

Renormalization of QED was also established at the one loop level for all relevant ranges of temperature and chemical potential [23,25–27].

The calculation of electron self energy at finite temperature is done up-to the two loop level since the electron mass shift has relevance to primordial nucleosynthesis at the time of BBN. Study of this aspect has acquired even more relevance in recent years since the observational probes such as WMAP had been providing data with unprecedented precision [28–31] for light element abundance parameters. Latest observational probes such as Planck and Herschel have now started providing observational data with further definitive accuracy.

Integrations, at two loop level, over the temperature dependent momenta have been reexamined and wherever needed are re-done for all the ranges of temperature that are relevant in QED. Two-loop electron self energy diagram with the one-loop vacuum polarization insertion as a subdiagram in Fig. 1(a) is omitted here because, as pointed out in Ref. [32] and also checked in Ref. [22], it contributes only to charge renormalization and has been included here for presenting all combinations expected. The divergences in Fig. 1(a) can be explicitly removed, however, by adding similar terms from Fig. 2(a).

Electron self energy in Figs. 1(b) and 1(c) is once again rechecked here at the two loop level, from the point of view of renormalization, with integration over hot loop momenta first, in the electron self energy diagrams and vice versa. The overlapping loops in Fig. 1(b) has (non-zero) real terms:

$$
\begin{aligned}
\Sigma^b(p) = e^4 \int \frac{d^4k}{(2\pi)^4} \int \frac{d^4l}{(2\pi)^4} N^b \Bigg[& \left\{ -\frac{\delta[(p-l)^2 - m^2] n_F(p-l)}{l^2 k^2 [(p-k)^2 - m^2][(p-k-l)^2 - m^2]} \right. \\
& \left. + \frac{\delta(l^2) n_B(l)}{k^2 [(p-l)^2 - m^2][(p-k)^2 - m^2][(p-k-l)^2 - m^2]} \right\} \\
& + 4\pi^2 \left\{ \frac{\delta(l^2) n_B(l) \delta(k^2) n_F(k) \delta\{(p-k-l)^2 - m^2\} n_F(p-k-l)}{[(p-k)^2 - m^2][(p-l)^2 - m^2]} \right. \\
& + \frac{\delta(l^2) n_B(l) \delta\{(p-k)^2 - m^2\} n_F(p-k) \delta\{(p-k-l)^2 - m^2\} n_F(p-k-l)}{k^2 [(p-l)^2 - m^2]} \\
& \left. + \frac{\delta(k^2) n_B(k) \delta\{(p-l)^2 - m^2\} n_F(p-l) \delta\{(p-k-l)^2 - m^2\} n_F(p-k-l)}{l^2 [(p-k)^2 - m^2]} \right\} \\
& + (l \leftrightarrow k) \text{ terms} \Bigg],
\end{aligned}
\tag{2}
$$

with

$$
\begin{aligned}
N^b = \big[& 2(p^2 - p \cdot k - p \cdot l + k \cdot l)(\slashed{p} - \slashed{k} - \slashed{l}) - m\{3p^2 + k^2 + l^2 - 2p \cdot k - 2p \cdot l \\
& - 6k \cdot l - 2\slashed{p}\slashed{k} + (3\slashed{k} - 2\slashed{p})\} - m^2(3\slashed{p} - 2\slashed{k} - 2\slashed{l}) + m^3 \big].
\end{aligned}
\tag{3}
$$

The terms in Eq. (2) have been integrated in detail separately. At two loop level, renormalization of the theory can be proven if hot integrals are also evaluated before the cold integrals on mass shell and added to the results for loop integrations done in the reverse order. If results from both of these combination of integration orders are not added up, the overlapping ultraviolet divergences do not cancel out exactly. This was not specifically noted in Ref. [22], where a particular order of integrations was not tracked down for the calculations of the wavefunction renormalization and therefore, integrations of variables was done arbitrarily. Inclusion of both the orders of integrations in this manner helps to handle the statistical effects in all possible ways. We demonstrate this, in the following, by writing down results from overlapping terms containing ultraviolet divergences arising from the terms with only one statistical distribution function each. If
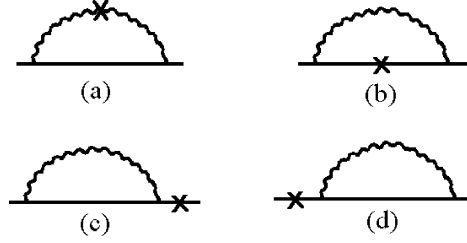
Fig. 2. Counter terms for two loop electron self energy.

integration over cold loop momenta is done before temperature dependent variables, one gets from the first two terms in Eq. (2) for the calculations of the wavefunction renormalization

$$\frac{-\alpha^2}{4\pi^3\varepsilon}\big[2\slashed{I} + 3(2m - \slashed{p})J_A + 2\slashed{J}_B\big].$$

Once hot loop energies are integrated out, the usual vacuum techniques of Feynman parametrization and dimensional regularization can be applied. On the other hand, if integration over hot loop momenta is done before cold momentum variables, we get:

$$\frac{-\alpha^2}{4\pi^3\varepsilon}[\slashed{I} + \slashed{J}_B].$$

The above two expressions are then added along with $(l \leftrightarrow k)$ combinations, rearranged and written in a concise form in the first line of Eq. (3). Therefore, overlapping divergences in Fig. 1(b) exactly get cancelled out by the terms on mass-shell to get:

$$\frac{3\alpha^2}{4\pi^3\varepsilon}[\slashed{I} + J_A + \slashed{J}_B]$$

coming from the diagrams in Fig. 2(b)–(d).

Integrations over both hot loop variables l and k, for the remaining terms in Eq. (2) have been redone in detail and combined appropriately including $(l \leftrightarrow k)$ combinations. They all finally give the electron self energy from the overlapping loops to be:

$$
\begin{aligned}
\Sigma_\beta^b(p) = \frac{\alpha^2}{2}\Bigg[& \frac{-1}{2\pi^3}\bigg\{\frac{1}{\varepsilon}\big[3\slashed{I} - (\slashed{p} + 6m)I_A + 3(2m - \slashed{p})J_A + 3\slashed{J}_B\big] \\
& - 3(\slashed{p} + 4m)I_A + 4\slashed{I} + (12m - 5\slashed{p})J_A + 2\slashed{J}_B\bigg\} \\
& + \sum_{n,r,s=1}^{\infty}(-1)^{r+1}e^{-r\beta E}\bigg\{\frac{3T^2}{4}\bigg[f_+(n,r)\Big\{mf_+(s,r)\Big(\frac{\boldsymbol{\gamma}\cdot\mathbf{p}}{|\mathbf{p}|^2}\Big)^2 - f_-(s,r)h_-(p,\gamma)\frac{\boldsymbol{\gamma}\cdot\mathbf{p}}{|\mathbf{p}|^2}\Big\} \\
& + \frac{I_B}{8\pi}\Big\{\Big(4 - \slashed{p}\frac{\boldsymbol{\gamma}\cdot\mathbf{p}}{|\mathbf{p}|^2}\Big)f_+(n,r) + \frac{(\slashed{p}+m)I_C}{8\pi}\Big\}\bigg] \\
& + (-1)^s\bigg[T^2\Big\{f_+(n,r)\Big[\frac{\boldsymbol{\gamma}\cdot\mathbf{p}}{|\mathbf{p}|^2}\Big(1 - 3m\frac{\boldsymbol{\gamma}\cdot\mathbf{p}}{|\mathbf{p}|^2}\Big)f_+(s,r) + 3h_-(p,\gamma)\frac{\boldsymbol{\gamma}\cdot\mathbf{p}}{|\mathbf{p}|^2}f_-(s,r)\Big] \\
& - \Big[\Big\{\frac{1}{m}h_-(p,\gamma) - 3m\Big(\frac{\boldsymbol{\gamma}\cdot\mathbf{p}}{|\mathbf{p}|^2}\Big)^2\Big\}f_+(s,r) - \frac{3}{m}h_+(p,\gamma)f_-(s,r)\Big]f_-(n,r)\Big\} \\
& - T\Big\{\Big[\Big\{\Big(5\slashed{p} + 3m^2\frac{\boldsymbol{\gamma}\cdot\mathbf{p}}{|\mathbf{p}|^2}\Big)\frac{\boldsymbol{\gamma}\cdot\mathbf{p}}{|\mathbf{p}|^2} - 12\Big\}f_+(n,r) + \frac{5\slashed{p}}{m}h_-(p,\gamma)f_-(n,r)\Big]\mathrm{Ei}_- \\
& - 3E\,\mathrm{Ei}_+\Big[\frac{1}{m}f_-(n,r)h_+(p,\gamma) - \frac{\boldsymbol{\gamma}\cdot\mathbf{p}}{|\mathbf{p}|^2}f_+(n,r)h_-(p,\gamma)\Big]\Big\} \\
& + \Big\{3h_-(p,\gamma)\frac{\boldsymbol{\gamma}\cdot\mathbf{p}}{v^2}f_+(n,r) - \frac{1}{m}f_-(n,r)\big[3|\mathbf{p}|^2 h_+(p,\gamma) - 5E\slashed{p}h_-(p,\gamma)\big]\Big\}\Big\{\frac{2e^{-r m\beta}}{m}\sinh sm\beta + \frac{1}{T}(r\,\mathrm{Ei}_+ + s\,\mathrm{Ei}_-)\Big\} \\
& - m\Big\{\frac{(r\,\mathrm{Ei}_+ - s\,\mathrm{Ei}_-)}{T} + \frac{2e^{-r m\beta}}{m}\cosh sm\beta\Big\}\Big\{f_-(n,r)\Big[h_-(p,\gamma) - 3m\Big(\frac{\boldsymbol{\gamma}\cdot\mathbf{p}}{|\mathbf{p}|^2}\Big)^2\Big] - \frac{m}{2}\frac{\boldsymbol{\gamma}\cdot\mathbf{p}}{|\mathbf{p}|^2}\Big(1 - 3m\frac{\boldsymbol{\gamma}\cdot\mathbf{p}}{|\mathbf{p}|^2}\Big)f_+(n,r)\Big\} \\
& - \Big\{2\gamma^0 T\Big[1 + \frac{T}{m}f_+(s,r)\Big] + \slashed{p}T\Big[\frac{2}{m}h_-(p,\gamma) - \frac{\boldsymbol{\gamma}\cdot\mathbf{p}}{|\mathbf{p}|^2}\Big]\Big\}f_-(s,r) + \big[E\,\mathrm{Ei}_+ - m\gamma^0\,\mathrm{Ei}_-\big] \\
& + \slashed{p}\Big[\frac{m^2}{2}\frac{\boldsymbol{\gamma}\cdot\mathbf{p}}{|\mathbf{p}|^2} + \frac{2E^2}{m}h_-(p,\gamma)\Big]\Big[\frac{e^{-m\beta(s+r)} - e^{-m\beta(r-s)}}{m} + \beta(r\,\mathrm{Ei}_+ - s\,\mathrm{Ei}_-)\Big]\frac{I_C}{8\pi}\bigg]\bigg\}\Bigg],
\end{aligned}
$$
(4)

where

$$f_{\pm}(n,r) = \left\{ \frac{1}{(n+r)} \pm \frac{1}{(n-r)} \right\}, \qquad f_{\pm}(s,r) = \left\{ \frac{1}{(s+r)} \pm \frac{1}{(s-r)} \right\}, \qquad h_{\pm}(p,\gamma) = \left(\gamma^0 \pm \frac{\boldsymbol{\gamma} \cdot \mathbf{p}}{v|\mathbf{p}|} \right),$$

$$\mathrm{Ei}_{\pm} = \mathrm{Ei}\big[-m\beta(r+s)\big] \pm \mathrm{Ei}\big[-m\beta(r-s)\big], \qquad I_B = 8\pi \sum_{r=1}^{\infty} (-1)^r \int_0^{\infty} \frac{dk}{k} e^{-r\beta(p-k)} n_B(k), \qquad I_C = 8\pi \sum_{r=1}^{\infty} (-1)^r \int_0^{\infty} \frac{dk}{k} e^{-r\beta k} n_B(k).$$

The non-vanishing real terms from loop within loop correction $\Sigma^c(p)$ in Fig. 1(c) are calculated from

$$\Sigma^c(p) = 4e^4 \int \frac{d^4q}{(2\pi)^4} \int \frac{d^4l}{(2\pi)^4} \big[q^2(\slashed{q}+\slashed{l}) - 2l\cdot q(\slashed{q}-2m) - m^2(3\slashed{q}+\slashed{l}) + 4m^3\big]$$

$$\times \Bigg[\frac{\delta(l^2)n_B(l)}{k^2[(p-l)^2-m^2][(p-k)^2-m^2][(p-k-l)^2-m^2]} $$

$$+ 4\pi^2 \Bigg\{ \frac{\delta(l^2)n_B(l)\delta(k^2)\delta\{(q-l)^2-m^2\}n_F(q-l)\delta(q_0-E_q)n_F(q)}{2E_q^2(q_0+E_q)(p-q)^2} $$

$$+ \frac{\delta(l^2)n_B(l)\delta(k^2)n_F(q-l)\delta\{(q-l)^2-m^2\}n_F(q)\delta'(q_0-E_q)}{2E_q^2(p-q)^2} $$

$$+ \frac{n_F(q)\delta(k^2)n_F(q-l)\delta\{(q-l)^2-m^2\}n_B(p-q)\delta(p-q)^2}{2E_q^2 l^2} \left[\frac{\delta(q_0-E_q)}{(q_0+E_q)} + \delta'(q_0-E_q) \right] \Bigg\} \Bigg], \tag{5}$$

with $q = p - k$. Carrying out all the integrations in Eq. (5) one by one and then combining them, we get

$$\Sigma_{\beta}^c(p) = \alpha^2 \Bigg\{ \frac{2T^2}{3m^2}(\slashed{p}-m) + mT \sum_{n,r,s=1}^{\infty} (-1)^{s+r} \Bigg[\Big\{ \beta(r+s)\,\mathrm{Ei}\big[-m\beta(r+s)\big] $$

$$+ \frac{e^{-m\beta(s+r)}}{m} \Big\} \Big\{ \frac{1}{(n-r)} \Big[\frac{2E}{m} + \gamma^0\Big(\frac{1}{2} - \frac{E^2}{m^2}\Big) + r\beta\Big(m - \frac{\slashed{p}}{2}\Big) \Big] + \frac{1}{(n-s)}\Big[h(p,\gamma) + m\frac{\boldsymbol{\gamma}\cdot\mathbf{p}}{|\mathbf{p}|^2} \Big] \Big\} $$

$$+ \frac{1}{2(n-r)} \Big\{ \frac{2}{m} - \frac{E\gamma^0}{m^2} + r\beta\Big[h(p,\gamma) + m\frac{\boldsymbol{\gamma}\cdot\mathbf{p}}{|\mathbf{p}|^2} \Big]\,\mathrm{Ei}\big[-m\beta(r+s)\big] \Big\} \Bigg] $$

$$- \frac{\pi T}{6|\mathbf{p}|} \sum_{n,r,s=1}^{\infty} (-1)^{r+1} e^{-n\beta E} \Big[h(p,\gamma)\Big\{ \big[1+(-1)^s\big] \frac{e^{-m\beta(r-n-s)}}{r-n-s} \Big\} $$

$$- T\frac{\boldsymbol{\gamma}\cdot\mathbf{p}}{|\mathbf{p}|^2} \frac{e^{-m\beta(r-n)}}{r-n} + \Big(2 - \frac{m\boldsymbol{\gamma}\cdot\mathbf{p}}{|\mathbf{p}|^2}\Big)\Big\{ m\beta(r-n)\,\mathrm{Ei}\big[-m\beta(r-n)\big] $$

$$- e^{-m\beta(r-n)} + \beta\big[1+(-1)^{1+s}\big]\mathrm{Ei}\big[-m\beta(r-n-s)\big] \Big\} \Big] \Bigg\}. \tag{6}$$

Fig. 1(c) gives only finite result, as was the case in Ref. [22] as well. The additional hot infrared divergences I_A, I_B, and I_C in Fig. 1(b) that appear at finite temperatures are appropriately removed in particle decay processes via bremsstrahlung emission and absorption effects [5,25]. Temperature acts as a regularization parameter for hot ultraviolet divergences. Thus after rearranging the finite terms we obtain temperature corrections to electron mass and wavefunction. Further, even for finite terms, in Eqs. (4) and (6), the integrations are redone in a manner that not only sufficiently eases the calculations but results are also simpler. This is obvious from the expressions of finite terms here as compared to those in Ref. [22].

3. The electron mass shift

To incorporate finite temperature effects in physical processes beyond tree level, one needs to have a consistent method of temperature dependent renormalization. As already mentioned, renormalizability of electron mass was done through the order by order cancellation of singularities up to two loop level even in Ref. [22] and redone here more explicitly. It can be checked that the second order in α correction is much smaller than the first order contribution so that the perturbative behavior is valid. The shift in the electron mass due to finite temperature effects is calculated here after we put together results from all the finite terms in electron self energy up-to second order in α using Eqs. (4) and (6). As electrons acquire temperature dependent (or thermal) mass from the medium, following Ref. [5], the physical mass of electron at one loop was obtained in Ref. [25] in generalized form, by writing

$$\Sigma(p) = A(p)E\gamma_0 - B(p)\vec{p}\cdot\vec{\gamma} - C(p),$$

where $A(p)$, $B(p)$, and $C(p)$ are the relevant coefficients. Taking inverse of the propagator with momentum and mass term separated as

$$S^{-1}(p) = (1-A)E\gamma^0 - (1-B)p\cdot\gamma - (m-C),$$

physical mass $m_{phy} = m + \delta m^{(1)} + \delta m^{(2)}$, was deduced by locating pole of the propagator $\frac{i(\not{p}+m)}{p^2-m^2+i\varepsilon}$. $\delta m^{(1)}$ and $\delta m^{(2)}$ is the shift in electron mass due to temperature effects at one and two loop level respectively. Using the same procedure, relative shift in electron mass at the two loop level was obtained [22]. On recombining similar summations and rearranging, the shift in electron mass becomes:

$$
\begin{aligned}
\frac{\delta m^{(2)}}{m} = 2\alpha^2 \sum_{r=1}^{\infty}\Bigg[& \frac{T^2}{m^2}\Bigg\{ \sum_{n=3}^{r+1}(-1)^{n+r+1}\frac{\pi m}{6Ev}\frac{e^{-\beta(rE+mn)}}{n} \\
& -\frac{3}{8}(-1)^r\frac{e^{-r\beta E}}{E^2v^2}\Bigg[\frac{9E^2}{2m^2}+6\sum_{s=3}^{r+1}\frac{1}{s}+4\sum_{n,s=3}^{r+1}\frac{1}{ns}+(-1)^{s-r}\Bigg\{\frac{9E}{m}\Bigg(3+4\sum_{s=3}^{r+1}\frac{1}{s}\Bigg) \\
& +2\Bigg(\frac{E^2v^2}{m^2}-3\Bigg)\Bigg(9+18\sum_{s=3}^{r+1}\frac{1}{s}+8\sum_{n,s=3}^{r+1}\frac{1}{ns}\Bigg)\Bigg\}\Bigg]+\frac{4}{E^2v^2}\Bigg\} \\
& -\frac{m^2}{\pi^2}c(m\beta)-\frac{T}{m}\Bigg\{\frac{\pi}{6Ev}\sum_{s=2}^{r+1}\sum_{n=1}^{s+1}\frac{e^{-\beta(rE+mn)}}{n}\Big[1-\{(-1)^{r+n}-(-1)^{s+n}\}\Big] \\
& +\Bigg[\{\text{Ei}(-m\beta)-\text{Ei}(-2m\beta)\}\Bigg\{\frac{9E}{4}\Bigg(\frac{E}{E^2v^2}-\frac{1}{m}\Bigg)+\Bigg(\frac{5E}{m}-21+\frac{E^2}{2m^2}\Bigg)\sum_{n=3}^{r+1}\frac{1}{n}\Bigg\} \\
& +\Bigg\{\frac{9}{4v^2}-\sum_{n=1}^{s+1}\sum_{s=3}^{r+1}\Bigg[1-E^2\Bigg(\frac{1}{2m^2}+\frac{3}{E^2v^2}\Bigg)+\frac{3E}{m}\Bigg]\Bigg\}(-1)^s\,\text{Ei}(-sm\beta)\Bigg] \\
& +e^{-rm\beta}\Bigg\{\Bigg[\frac{9E}{2v^2}+2\Bigg(\frac{3E}{v^2}+\frac{3E^2v^2}{m}-5E\Bigg)\sum_{n=3}^{r+1}\frac{1}{n}\Bigg]\sum_{s=1}^{\infty}\sinh sm\beta-\frac{3m^3}{E^2v^2}\Bigg(\frac{3}{4}-\sum_{n=3}^{r+1}\frac{1}{n}\Bigg)\sum_{s=1}^{\infty}\cosh sm\beta\Bigg\}\Bigg\} \\
& +\Bigg\{\frac{9m}{4E^2v^2}\Bigg(E^3+\frac{m^3}{2}\Bigg)+\Bigg[\frac{3m}{E^2v^2}(E^3+m^3)+5mE-3E^2v^2\Bigg]\sum_{n=3}^{r+1}\frac{1}{n}\Bigg\}\{\text{Ei}(-m\beta)-2\,\text{Ei}(-2m\beta)\} \\
& -\sum_{n=3}^{r+1}\Bigg\{\sum_{s=1}^{r+1}\frac{(-1)^s}{n}\Bigg[\frac{m^2r}{2}e^{-sm\beta}+\Bigg\{sE\Bigg(2m-\frac{E^2}{m}\Bigg)+\frac{m^2(s-r)}{2}\Bigg\}\text{Ei}(-sm\beta)\Bigg] \\
& -\frac{\pi m^2}{3Ev}\Bigg[e^{-\beta rE}(-1)^{n+r}(n+1)-\sum_{s=2}^{r+1}(-1)^{n+s}\Bigg]\text{Ei}(-nm\beta)\Bigg\}\Bigg].
\end{aligned}
$$
(7)

These self energy and self mass corrections to electrons are of significance for primordial abundances of light elements. During primordial nucleosynthesis era, when temperature was suitable enough to synthesize nuclei of light elements ($T \sim 0.1$–10 MeV), nucleon capturing led to certain bounds on light elemental nuclei abundances, specifically ^{4}He abundance parameter Y which is expected to be 0.25 for correspondence with BBN while the measured value, from all the possibilities combined, is slightly less (around 0.24). These results for $\frac{\delta m}{m}$ are applied to determine the corrections in ^{4}He abundance [10–13,33] as related to the relative mass shift through

$$
\Delta Y = 0.2\frac{\Delta\tau}{\tau} = -0.2\frac{\Delta\lambda}{\lambda} = 0.04\Bigg(\frac{m}{T}\Bigg)^2\frac{\delta m}{m}
$$
(8)

where $\frac{\Delta\tau}{\tau}$ is relative change in neutron half life and $\frac{\Delta\lambda}{\lambda}$ is relative change in neutron decay rate.

For one loop corrections estimated in Ref. [33] $\Delta Y = 0.4 \times 10^{-3}$ at $T \sim m$ and falls to 0.3×10^{-3} at $T \sim m/3$. For example, with energies around 1 MeV, $\Delta Y = 0.31 \times 10^{-4}$ from one particle irreducible diagram, considered in detail in [34], is just one order of magnitude lesser (~ 10)% compared to the one loop contribution. This can be compared with other data which shows that if BBN is correct, Monte Carlo simulations give $Y_p = 0.2476 \pm 0.0004$ [35] and through CMB predictions $Y_p = 0.24819^{+0.00029}_{-0.00040} \pm 0.0006$ (syst.) [36]. It must be noted that at order α^2 temperature correction though small is, however, not negligible to modify ΔY.

4. Wavefunction renormalization

With finite temperature background in the real-time formalism, since Lorentz invariance is broken, momentum independent renormalization constant in vacuum is no longer sufficient. Donoghue and Holstein used temperature dependent propagators to modify electron mass as well as the spinors accordingly [5]. Wave function renormalization for the generalized temperatures does not exist in literature, for two loop corrections. Using the reviewed expression for the electron self energy obtained in Eqs. (4) and (6) relation for wave function renormalization constant is derived by taking $Z_2^{-1} = \frac{\partial\Sigma}{\partial\not{p}}$. This comes out to be

$$Z_2^{-1} = 1 - \alpha \left[\frac{1}{4\pi}\left(\frac{3}{\varepsilon} - 4\right) + \frac{5}{\pi}b(m\beta) + \frac{I_A}{4\pi^2} - \frac{T^2}{\pi v E^2}\ln\frac{1+v}{1-v}\left\{\frac{\pi^2}{6} - c(m\beta) + m\beta a(m\beta)\right\}\right]$$

$$- \alpha^2 \left[\frac{1}{4\pi^3}\left\{\frac{3}{\varepsilon}(I_A + J_A) + (3I_A + 5J_A)\right\} - \frac{2T^2}{3\pi^3 m^2} + \frac{m}{8\pi}\sum_{n,r,s=1}^{\infty}(-1)^{s+r}\left\{r\left[\frac{e^{-m\beta(s+r)}}{m} - \beta(r+s)\,\text{Ei}\{-m\beta(r+s)\}\right]\right\}\right]$$

$$+ \frac{1}{8}\sum_{n,r,s=1}^{\infty}(-1)^r T\left\{e^{-r\beta E}\left[f_+(s,r)\frac{\boldsymbol{\gamma}\cdot\mathbf{p}}{E^2 v^2} + h(p,\gamma)\left\{f_-(n,r)\frac{I_C}{8\pi} - f_-(s,r)\right\} + f_+(n,r)\frac{\boldsymbol{\gamma}\cdot\mathbf{p}}{E^2 v^2}\frac{I_B}{8\pi} - \frac{I_B I_C}{64\pi^2}\right]$$

$$+ \left[\left\{5\frac{\boldsymbol{\gamma}\cdot\mathbf{p}}{E^2 v^2}f_+(n,r) - \frac{5}{m}h(p,\gamma)f_-(n,r)\right\}\text{Ei}_- + \frac{5E}{m^2}h(p,\gamma)f_-(n,r)\left\{\frac{2e^{-rm\beta}}{m}\sinh sm\beta + \beta(r\,\text{Ei}_+ + s\,\text{Ei}_-)\right\}\right.$$

$$+ \left.\left\{\frac{2}{m}h(p,\gamma) - \frac{\boldsymbol{\gamma}\cdot\mathbf{p}}{E^2 v^2}\right\}f_-(s,r)\right]\right\} + \left\{\frac{m^2}{2}\frac{\boldsymbol{\gamma}\cdot\mathbf{p}}{E^2 v^2} + \frac{2E^2}{m}h(p,\gamma)\right\}\left\{\frac{2e^{-rm\beta}}{m}\sinh sm\beta + \beta(r\,\text{Ei}_+ - s\,\text{Ei}_-)\right\}\frac{I_C}{8\pi}\right]. \tag{9}$$

From this expression for Z_2^{-1}, not only the behavior at intermediate temperatures $T \sim m$ can be extracted but ranges of high temperature $T \gg m$, low temperature $T \ll m$, can be also retrieved from it, as limiting cases.

5. Results and summary

We have demonstrated explicitly the cancellation of overlapping hot and cold divergences in Fig. 1(b) with the counter terms from Figs. 2(b)–2(d). For this, the results from an integration of hot loops before the cold ones were combined with those from the reverse order of integration. This has been explicitly checked for the first time, leading to a conclusion that addition of both the possible combinations of hot and cold loop momenta integrations are a must so that all the statistical effects are appropriately incorporated.

Rewriting electron self energy expressions in QED at the two loop level that were presented in Ref. [22], one obtains a modified expression for relative change in electron mass at the two loop level in Eq. (4). Previously calculated self-mass correction terms are redone for simplicity and conciseness, wherever required, for all the possible ranges of temperature. From these corrections one can then retrieve results for the temperature ranges of interest here, classified as, high temperature $T \gg m$ (having $m\beta \to 0$ with $e^{-m\beta}$ falling off exponentially as compared to $\frac{T^2}{m^2}$), low temperature $T \ll m$ (with fermions contribution negligible) and intermediate temperatures $T \sim m$ (by taking $m\beta \to 1$).

Self energy and self mass corrections to electron are of significance for primordial abundances since they get dynamically generated mass due to plasma screening effect. During the era of primordial nucleosynthesis, when temperature was suitable enough to synthesize nuclei of light elements, it led to bounds on ^{4}He abundance. Order α^2 temperature correction are not negligible and can serve as one of the sources of input for modification in ΔY.

We calculated here, for the first time, using thermal contributions in the generalized form of temperature, wavefunction renormalization constant up to second order in α. Fermions do not pick any contribution from the heat bath at low temperature. Therefore, the second order in α corrections to electron self energy at low temperature can be retrieved as a limiting case that contains contribution from hot photons only. Thus wave function renormalization constant up-to two loops in Eq. (6) in the limit $T \ll m$ reduces to

$$Z_2^{-1} \xrightarrow{T \ll m} 1 + \frac{\alpha}{4\pi}\left(4 - \frac{3}{\varepsilon}\right) - \frac{\alpha}{4\pi^2}\left(I_A - \frac{I^0}{E}\right) - \frac{\alpha^2}{4\pi^2}\left(3 + \frac{1}{\varepsilon}\right)I_A + \frac{2\alpha^2 T^2}{3\pi^2 m^2}, \tag{10}$$

which is the same as that in Ref. [37]. The high temperature limit for wave function renormalization constant gives:

$$Z_2^{-1} \xrightarrow{T \gg m} 1 - \alpha\left[\frac{2I_A}{\pi} + \frac{1}{4\pi}\left(\frac{3}{\varepsilon} - 4\right) + \frac{4\pi T^2}{3}\right] - \alpha^2\left[\frac{1}{4\pi^3}\left\{\frac{3}{\varepsilon}(I_A + J_A) + (3I_A + 5J_A) - \frac{8T^2}{3m^2}\right\}\right.$$

$$+ \frac{1}{8}\sum_{n,r,s=1}^{\infty}(-1)^r T\left\{e^{-r\beta E}\left[f_+(s,r)\frac{\boldsymbol{\gamma}\cdot\mathbf{p}}{E^2 v^2} - \frac{I_B I_C}{64\pi^2} + h(p,\gamma)\left\{f_-(n,r)\frac{I_C}{8\pi} - f_-(s,r)\right\} + f_+(n,r)\frac{\boldsymbol{\gamma}\cdot\mathbf{p}}{E^2 v^2}\frac{I_B}{8\pi}\right.\right.$$

$$+ \left.\left.\left\{\frac{2}{m}h(p,\gamma) - \frac{\boldsymbol{\gamma}\cdot\mathbf{p}}{E^2 v^2}\right\}f_-(s,r)\right]\right\}\right]. \tag{11}$$

Eq. (8) shows that the leading contribution in this range of temperature, $T \gg m$, at the two loop level is $\frac{2T^2}{3m^2}$. It is worth mentioning that thermal corrections, at second order in α, to wavefunction renormalization constant at extreme temperatures ($T \ll m$ and $T \gg m$) are still proportional to $\frac{T^2}{m^2}$ as in case of the self mass of electron. The self-energy expression for intermediate temperatures is somewhat different from the one obtained earlier [22]. Calculations around $T \sim m$ for mass and wavefunction renormalization constants though still cumbersome at the two-loop level, are much simpler than those in Ref. [22].

Two loop fermion self energy in QED has been calculated in detail recently [38] using the hard thermal loop (HTL) resummation introduced by Braaten and Pisarski [39–41]. As far as the renormalization is concerned, HTL do not affect it [38]. Hence Z_2 does not get any contribution from HTL here.

Renormalizability of the theory at finite temperature is explicitly established up to order α^2 and holds through order by order cancellation of singularities. This provides a platform to include general effects due to chemical potential in hot and dense background later on. With an experience of including chemical potential at one loop level, in real time formulation [23,26,27], it is foreseen that two loop

self energy calculations will be much more complicated but are still worth-doing to develop a calculational technique for high density hot plasmas, even in case of superfluids inside the cores of neutron stars [42]. The modified wavefunction is expected to affect finite temperature contributions to electroweak processes [43] as well as neutrino magnetic moments [44] up to the two loop level.

Acknowledgements

References

[1] E.P. Liang, S.C. Wilks, M. Tabak, Phys. Rev. Lett. 81 (1998) 4887.
[2] B. Shen, J. Meyer-ter-Vehn, Phys. Rev. E 65 (2001) 016405.
[3] M.H. Thoma, Eur. Phys. J. D 55 (2009) 271;
    M.H. Thoma, Rev. Mod. Phys. 81 (2009) 959.
[4] H.A. Weldon, Phys. Rev. D 26 (1982) 1394.
[5] J.F. Donoghue, B.R. Holstein, Phys. Rev. D 28 (1983) 340;
    J.F. Donoghue, B.R. Holstein, Phys. Rev. D 29 (1983) 3004 (Erratum).
[6] P. Landsman, Ch.G. Weert, Phys. Rep. 145 (1987) 141.
[7] D.A. Dicus, E.W. Kolb, A.M. Gleeson, E.C.G. Sudarshan, V.L. Teplitz, M.S. Turner, Phys. Rev. D 26 (1982) 2694.
[8] J.-L. Cambier, J.R. Primack, M. Sher, Nucl. Phys. B 209 (1982) 372.
[9] J.F. Donoghue, B.R. Holstein, R.W. Robinett, Ann. Phys. (N.Y.) 164 (1985) 233.
[10] A.E. Johansson, G. Peresutti, B.S. Skagerstam, Nucl. Phys. B 278 (1986) 324.
[11] W. Keil, Phys. Rev. D 40 (1989) 1176.
[12] R. Baier, E. Pilon, B. Pire, D. Schiff, Nucl. Phys. B 336 (1990) 157.
[13] W. Keil, R. Kobes, Physica A 158 (1989) 47.
[14] M. LeBellac, D. Poizat, Z. Phys. C 47 (1990) 125.
[15] T. Altherr, P. Aurenche, Phys. Rev. D 40 (1989) 4171.
[16] R.L. Kobes, G.W. Semeneff, Nucl. Phys. B 260 (1985) 714;
    R.L. Kobes, G.W. Semeneff, Nucl. Phys. B 272 (1986) 329.
[17] R.F. Sawyer, Phys. Rev. D 53 (1996) 4232.
[18] I.A. Chapman, Phys. Rev. D 55 (1997) 6287.
[19] S. Esposito, G. Mangano, G. Miele, O. Pisanti, Phys. Rev. D 58 (1998) 105023.
[20] V.V. Klimov, Sov. J. Nucl. Phys. 33 (1981) 934;
    L. Dolan, R. Jackiw, Phys. Rev. D 9 (1974) 3320;
    S. Weinberg, Phys. Rev. D 9 (1974) 3357;
    C. Bernard, Phys. Rev. D 9 (1974) 3312.
[21] Mahnaz Qader Haseeb, Samina S. Masood, K. Ahmed, Phys. Rev. D 44 (1991) 3322.
[22] Mahnaz Qader Haseeb, Samina S. Masood, K. Ahmed, Phys. Rev. D 46 (1992) 5633.
[23] K. Ahmed, Samina S. Masood, Ann. Phys. (N.Y.) 207 (1991) 460.
[24] Samina S. Masood, Mahnaz Q. Haseeb, Int. J. Mod. Phys. A 23 (2008) 4709.
[25] K. Ahmed, Samina Saleem Masood, Phys. Rev. D 35 (1987) 1861.
[26] K. Ahmed, Samina Saleem Masood, Phys. Rev. D 35 (1987) 4020.
[27] Samina S. Masood, Phys. Rev. D 44 (1991) 3943;
    Samina S. Masood, Phys. Rev. D 47 (1993) 648.
[28] G. Hinshaw, et al., Astrophys. J. Suppl. 180 (2009) 225.
[29] C.L. Bennett, et al., Astrophys. J. Suppl. 192 (2011) 17.
[30] G. Steigman, Primordial nucleosynthesis after WMAP, chemical abundances in the universe: Connecting first stars to planets, in: K. Cunha, M. Spite, B. Barbuy (Eds.), Proc. IAU Sympos., vol. 265, 2009, pp. 119–138.
[31] G. Steigman, Int. J. Mod. Phys. E. 15 (2005) 1;
    G. Steigman, Annu. Rev. Nucl. Part. Sci. 57 (2007) 463.
[32] D.A. Dicus, D. Down, E.W. Kolb, Nucl. Phys. B 223 (1983) 525.
[33] S. Saleem, Phys. Rev. D 36 (1987) 2602.
[34] Mahnaz Q. Haseeb, Omair Sarfaraz, Primordial nucleosynthesis and finite temperature QED, Journal of Cosmology and Astrophysics, May 15, 2011, submitted for publication.
[35] A. Coc, E. Vangioni, J. Phys.: Conf. Ser. 202 (2010) 012001.
[36] D.N. Spergel, et al., Astrophys. J. Suppl. 170 (2007) 377.
[37] Mahnaz Q. Haseeb, Samina S. Masood, Chin. Phys. C 35 (2011) 608.
[38] E. Mottola, Z. Szép, Phys. Rev. D 81 (2010) 025014.
[39] E. Braaten, R.D. Pisarski, Nucl. Phys. B 337 (1990) 569.
[40] E. Braaten, R.D. Pisarski, Phys. Rev. D 42 (1990) 2156.
[41] R.D. Pisarski, Phys. Rev. Lett. 63 (1989) 1129.
[42] D. Page, et al., Phys. Rev. Lett. 106 (2011) 081101.
[43] Mahnaz Qader Haseeb, Samina S. Masood, Phys. Rev. D 46 (1992) 5110.
[44] Samina S. Masood, Phys. Rev. D 48 (1993) 3250.